Acta Cryst. (1979). A**35**, 789–795

X-ray Diffraction Study of $Zr(Ca,Y)O_{2-x}$.
I. The Average Structure

By M. Morinaga and J. B. Cohen

Department of Materials Science and Engineering, The Technological Institute, Northwestern University, Evanston, Illinois 60201, *USA*

and J. Faber Jr

Materials Science Division, Argonne National Laboratory, Argonne, Illinois 60439, *USA*

(*Received* 8 *January* 1979; *accepted* 25 *April* 1979)

Abstract

Integrated X-ray intensities of Bragg peaks were observed from single crystals of $Zr_{0.866}Ca_{0.134}O_{1.866}$ and $Zr_{0.786}Y_{0.214}O_{1.893}$ in the disordered state. There are displacements of oxygen ions (characterized by $\Delta/a \sim 0.05$) from the ideal positions of the fluorite structure along ⟨100⟩ directions similar to those that occur on ordering below 1273 K and related to the cubic to tetragonal transition in pure ZrO_2. These displacements are not related to anharmonicity, at least to fourth-order terms. In addition, there are small displacements of the cations ($\Delta/a \sim 0.015$) in ⟨111⟩ directions in the yttria-stabilized zirconia.

Introduction

$Zr(Ca)O_{2-x}$ and $Zr(Y)O_{2-x}$ are excellent conductors of O^{2-} ions at temperatures above 1173 K, and are, therefore, important solid electrolytes (Etsell & Flengas, 1970; Roth, 1975). These materials have fluorite-type structures, large concentrations of oxygen vacancies, and are stable in the cubic phase over wide ranges of composition and temperature (Etsell & Flengas, 1970). There is, however, a large difference in the reported regions of stability; Carter & Roth (1963, 1968) found that $Zr(Ca)O_{2-x}$ is stable in the range $0.10 < x < 0.19$ at 1673 K. Sardi (1969) indicated that $Zr(Y)O_{2-x}$ is stable in the range $0.07 < x < 0.29$, with this range being almost independent of temperature.

There is interest in the order–disorder transformation in these materials (*e.g.* Carter & Roth, 1963, 1968; Steele & Fender, 1974; Allpress & Rossel, 1975; Allpress, Rossel & Scott, 1975; Hudson & Moseley, 1976; Faber, Mueller & Cooper, 1978). Neutron diffraction studies of $Zr(Ca)O_{2-x}$ in the disordered and ordered states were first reported by Carter & Roth (1963, 1968). They suggested that above the transition (in the disordered state) there is a displacement of the oxygen ions from the ideal fluorite lattice sites in ⟨111⟩ directions with the magnitude of displacements reported to be 0·2–0·3 Å. The order–disorder transition occurs at ~1273 K and these authors inferred from their measurements that the ordering involved cooperative motions of the oxygen ions in ⟨111⟩ directions. In contrast to these results, Steele & Fender (1974) reported that in the disordered state of $Zr(Y)O_{2-x}$ there is a displacement of oxygen ions along ⟨100⟩ directions.

Allpress, Rossel & Scott (1975) have suggested a model for ordered $CaZr_4O_9$ (below 1273 K) from X-ray measurements with powders, but they could find no evidence for anion displacements from ideal positions. More recently, Faber, Mueller & Cooper (1978) interpreted neutron scattering from ordered single crystals of both $Zr(Ca)O_{1.85}$ and $Zr(Y)O_{1.91}$ in terms of internal deformation waves on the oxygen sublattice, with an amplitude of ~0·23 Å; each ion is displaced parallel or anti-parallel to ⟨100⟩ directions, collectively on {110} planes.

In all the previous studies (except that by Faber, Mueller & Cooper, 1978), powder methods were employed, limiting the accuracy of detecting any displacements, since only a few peaks, often at low $\sin\theta/\lambda$, are generally involved. In our experiments, integrated X-ray intensities of Bragg peaks were measured with single crystals of $Zr_{0.866}Ca_{0.134}O_{1.866}$ and $Zr_{0.786}Y_{0.214}O_{1.893}$. Structural refinements by conventional methods were employed to reveal the average structures.

Experimental methods

Well-characterized crystals were used in our experiments. Laue photographs showed that the crystals had compositions within the cubic solid solution phase field and that the crystals were single. The dopant concentrations (Ca or Y) were checked by X-ray

0567-7394/79/050789-07$01.00

fluorescence with the following results for the compositions: $Zr_{0.87}Ca_{0.13}O_{1.87}$ and $Zr_{0.79}Y_{0.21}O_{1.89}$, where we have assumed an oxygen vacancy model. Small portions of the crystals were ground to powder and lattice parameter determinations gave more exact compositions (see Carter & Roth, 1968 and Steele & Fender, 1974 for relations between compositions and lattice parameter). The crystals were heat-treated in air at 1673 K for 2·5 h (to avoid the interstitials detected at 2073 K by Diness & Roy, 1965) and then rapidly cooled (by turning off the furnace power and removing the crystals at 1523 K).* These had plate-like geometry, with faces much larger than the X-ray beam, $\simeq$5–7 by 8–11 mm. As only χ, Φ were employed to align various reflections in the symmetric ($\omega = 0$) orientation, no absorption corrections were employed. To confirm that there was no long-range order present, 20 min counts at 0·1° intervals were made in the vicinity of the 211 superlattice peak, and no reflection was detected. (The ratio of this peak to a 111 fundamental peak is $\sim 3 \times 10^{-3}$ (Roth, 1975) and the 111 peak was $\simeq 10^4$ Hz so the 211 superlattice peak would have easily been detected.)

Intensities were collected on a GE diffractometer equipped with a quarter-circle goniostat, a scintillation detector, pulse height discriminator, and controlled by a mini computer (Richesson, Morrison, Cohen & Paavola, 1971). Mo $K\alpha$ radiation was employed, monochromated by a pyrolitic graphite crystal in the incident beam, bent to focus at the detector normal to the diffraction plane. Integrations were obtained by θ–2θ step scans in increments of 0·02° 2θ, which were repeated automatically until the statistical error of the (net) intensity above background was $\leq$2%, for $Zr(Ca)O_{2-x}$ and $\leq$3% for $Zr(Y)O_{2-x}$. (The background was assumed to be linear and values on the low and high angle sides of each peak were averaged.) For yttria-stabilized zirconia, Y fluorescence caused a troublesome background even though a monochromator was employed. To improve the statistics of the net intensity, a Ni foil 0·035 mm thick was placed in front of the detector, which reduced the Mo $K\alpha$ radiation to 23% of its original value while reducing the background to 13%.

The integrated intensities were corrected for the Lorentz–polarization factor, assuming an ideally imperfect monochromator. Some 82–83 peaks were examined for each crystal, most of which were between 20 and 130° 2θ. It was assumed that the space group was $Fm3m$ in accord with all previous studies, and only independent reflections were measured. Several strong peaks at low angles were not analyzed because of extinction and uncertainty in corrections due to the measured dead time, $\sim$13 μs (Schwartz & Cohen, 1977). The contribution of temperature diffuse scattering to the measured intensities was not subtracted, as there are no available data on the elastic constants for these materials.

Results

(i) $ln(I/|F_c|^2)$ vs $sin^2\,\theta/\lambda^2$

$Ln(I/|F_c|^2)$ *vs* $(\sin^2\theta/\lambda^2)$ for $Zr(Ca)O_{2-x}$ and $Zr(Y)O_{2-x}$ are shown in Fig. 1(*a*) and (*b*) respectively, where I is the measured intensity after corrections, F_c is the calculated structure factor (without displacement or any Debye–Waller factor) and λ is the wavelength of

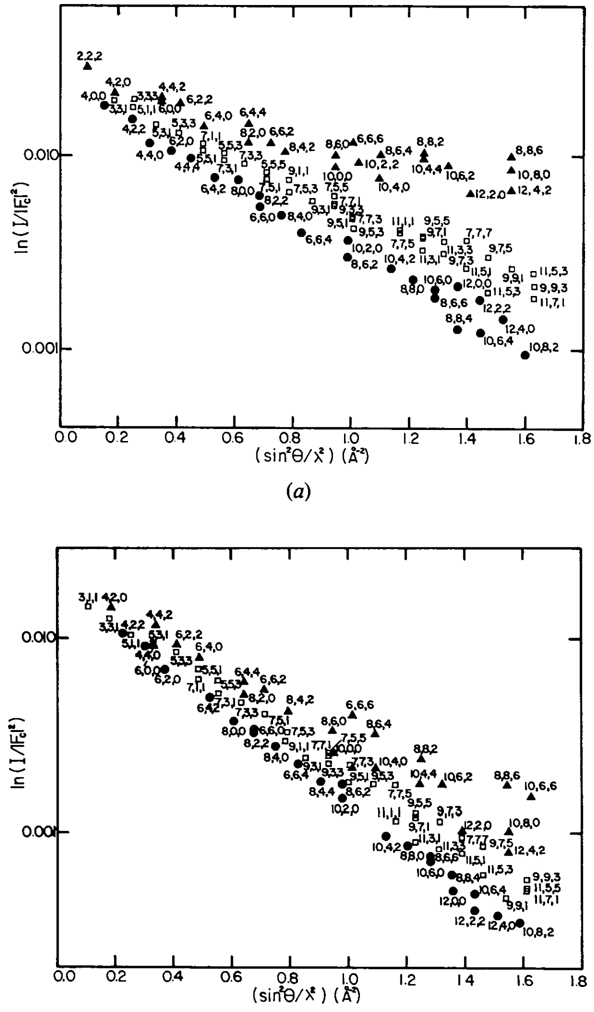

(*a*)

(*b*)

Fig. 1. $\ln(I/|F_c|^2)$ *vs* $(\sin^2\,\theta/\lambda^2)$ for (*a*) $Zr(Ca)O_{2-x}$ and (*b*) $Zr(Y)O_{2-x}$. ▲ h,k,l all even, $h + k + l = 4n + 2$; □ h,k,l all odd; ● h,k,l all even, $h + k + l = 4n$.

---

* This temperature is well above the ordering reaction at 1273 K; because this reaction requires 400–1000 h to produce appreciable order at 1223 K, the crystals were considered disordered.

X-rays. This structure factor can be simplified as follows:

$$h,k,l \text{ all odd: } F_c = 4\langle f_C\rangle, \tag{1a}$$

h,k,l all even,

$$h+k+l=4n: F_c = 4\langle f_C\rangle + 8\langle f_A\rangle, \tag{1b}$$

h,k,l all even,

$$h+k+l=4n+2: F_c = 4\langle f_C\rangle - 8\langle f_A\rangle, \tag{1c}$$

where $\langle f_C\rangle$ and $\langle f_A\rangle$ are the average scattering amplitudes of cations and anion, *i.e.* $\langle f_C\rangle = X_{\rm Zr} f_{\rm Zr} + (1 - Z_{\rm Zr}) f_{\rm Ca\,(or\,Y)}$ and $\langle f_A\rangle = X_{\rm O} f_{\rm O}$. Here, X_i is the occupation factor of the i ions on each sublattice and f_i is the associated atomic scattering factor. The values of $f_{\rm Zr}$, $f_{\rm Ca}$ and $f_{\rm Y}$ were taken from *International Tables for X-ray Crystallography* (1974), assuming that the ionic states were $\rm Zr^{4+}$, $\rm Ca^{2+}$, and $\rm Y^{3+}$. The value of $f_{\rm O}$ was taken from Tokonami (1965) assuming that the ionic state was $\rm O^{2-}$. An anomalous dispersion correction for Mo $K\alpha$ radiation was taken into account for all the elements (*International Tables for X-ray Crystallography*, 1974).

From Fig. 1(*a*) and (*b*), it is clear that there are three separate groups of reflections depending on reflection type, as in (1), and it is apparent from these formulae that this is due to the difference in the contribution of oxygen ions to F, despite the fact that its scattering factor is much smaller than that of the cations. The individual temperature factors of the cations and the anion are so different that one overall temperature factor is clearly not appropriate (note the curvature in these plots).

A least-squares refinement was carried out employing the *ORFLS* computer program (Busing, Martin & Levy, 1960, modified by Ibers). The unweighted and weighted R values were calculated, following the definitions:

$$\text{unweighted } R = \frac{\sum(|F_o| - |F_c|)}{\sum |F_o|}, \tag{2a}$$

and

$$\text{weighted } R = \left[\frac{\sum W_i(|F_o| - |F_c|)^2}{\sum W_i |F_o|^2}\right]^{1/2}, \tag{2b}$$

where F_o is the observed structure factor and W_i is the weighting factor for each observation, as suggested by Corfield, Doedens & Ibers (1967).

In the fluorite-type structure (space group $Fm3m$), the cation and anion sites are located as follows:

$$(000, \tfrac{1}{2}\tfrac{1}{2}0, \tfrac{1}{2}0\tfrac{1}{2}, 0\tfrac{1}{2}\tfrac{1}{2}) +$$

cation sites: $4(a)\ m3m\ 0,0,0;$

anion sites: $8(c)\ \bar{4}3m\ \ \tfrac{1}{4},\tfrac{1}{4},\tfrac{1}{4};\ \tfrac{3}{4},\tfrac{3}{4},\tfrac{3}{4};$

interstitial sites: $4(b)\ m3m\ \tfrac{1}{2},\tfrac{1}{2},\tfrac{1}{2}.$

Diness & Roy (1965) suggested that there are interstitial cations (but no vacancies) in $\rm Zr(Ca)O_{2-x}$, if it is quenched from high temperatures (2073 K) but vacant anion sites if quenched from 1873 K. To examine the possibility of interstitials in $\frac{1}{2}\frac{1}{2}\frac{1}{2}$ sites, R values were calculated and compared with that of a model with anion vacancies without any interstitial cations. In both cases the concentration of defects was taken to satisfy the overall composition. The refinements were carried out with three variables (the scale factor and individual temperature factors for the cations and anion). The results given in Table 1 were obtained.

Table 1. *R values for different refinements*

	Interstitial cation model		Anion vacancy model without any interstitial cations	
	Ordinary R	Weighted R	Ordinary R	Weighted R
$\rm Zr(Ca)O_{2-x}$	7·79%	9·20%	3·94%	6·11%
$\rm Zr(Y)O_{2-x}$	6·52%	9·09%	3·51%	6·50%

Thus, there do not appear to be any appreciable numbers of interstitial cations. In addition, no excess electron density appeared at interstitial positions in difference electron density maps (to be presented below). When the refinement is on these variables, the expected R values are 1% for $\rm Zr(Ca)O_{2-x}$ and 1·5% for $\rm Zr(Y)O_{2-x}$ (Hamilton, 1965*a*).

The temperature factors for the anion-vacancy model are as follows: B_C = 0·803 (16) Å^2, $B_{\rm O}$ = 2·890 (160) Å^2 for $\rm Zr(Ca)O_{2-x}$, and B_C = 1·120 (14) Å^2, $B_{\rm O}$ = 2·170 (87) Å^2 for $\rm Zr(Y)O_{2-x}$. As might be anticipated from the large differences in slopes for the various index sets in Fig. 1, the temperature factor of the oxygen ions is very high compared to that of the cations. This high value suggests that there are large displacements of oxygen ions not accounted for, as proposed by Carter & Roth (1968) and Steele & Fender (1974).

(ii) *Model of* $\langle 111\rangle$ *displacement of oxygen ions*

Carter & Roth (1968) suggested that each oxygen ion in the disordered phase is replaced statistically at one of four equivalent sites displaced along the $\langle 111\rangle$ directions. The magnitude of the displacement was estimated to be 0·2–0·3 Å, and almost independent of composition (X) in $\rm Zr(Ca)O_{2-x}$. To test for this displacement, the refinement was carried out on the scale factor and the two isotropic temperature factors for a series of specific displacements of oxygen ions along the $\langle 111\rangle$ directions. The results are given in Fig. 2(*a*) for $\rm Zr(Ca)O_{2-x}$ and (*b*) for $\rm Zr(Y)O_{2-x}$. Both the ordinary and weighted R values increase monotonically with increasing magnitude of the $\langle 111\rangle$ displacement. The significance test discussed by Hamilton (1965*b*) was applied to the weighted R values (see Fig.

2). With a 95% confidence level, it is concluded that the displacement proposed by Carter & Roth (1968) does not occur in either $Zr(Ca)O_{2-x}$ or $Zr(Y)O_{2-x}$. As we shall see, this conclusion is clearly illustrated by the difference electron density maps.

(iii) *Difference electron density maps*

The difference electron density, $\Delta\rho$, is defined as the observed electron density (ρ_o) minus the calculated one (ρ_c) (*e.g.* see Buerger, 1960). In such a map, a positive peak requires the addition of electrons (or ions), whereas a negative peak requires the removal of electrons (or ions). Such maps were made by calculating the structure factor with the two isotropic temperature factors of the cation and anion from refinements described in § (i). The results are given in Fig. 3(*a*) for $Zr(Ca)O_{2-x}$ and 3(*b*) for $Zr(Y)O_{2-x}$ respectively (the sections shown have $z = \frac{1}{4}$).

There are large positive peaks near an oxygen site [$\Delta\rho \simeq 2{\cdot}56$ e Å^{-3} for $Zr(Ca)O_{2-x}$ and $1{\cdot}46$ e Å^{-3} for $Zr(Y)O_{2-x}$]. It is apparent that displacements of oxygen ions occur along $\langle 100 \rangle$ directions, not $\langle 111 \rangle$ directions. This agrees with the suggestions of Steele & Fender (1974) for $Zr(Y)O_{2-x}$. Moreover, no extra electron density peak at ($\frac{1}{2}\frac{1}{2}\frac{1}{2}$) was detected, confirming that there are no interstitial cations. The slight positive peak at the normal oxygen position for $Zr(Y)O_{2-x}$ implies that there are fewer displaced anions in this material than in $Zr(Ca)O_{2-x}$.

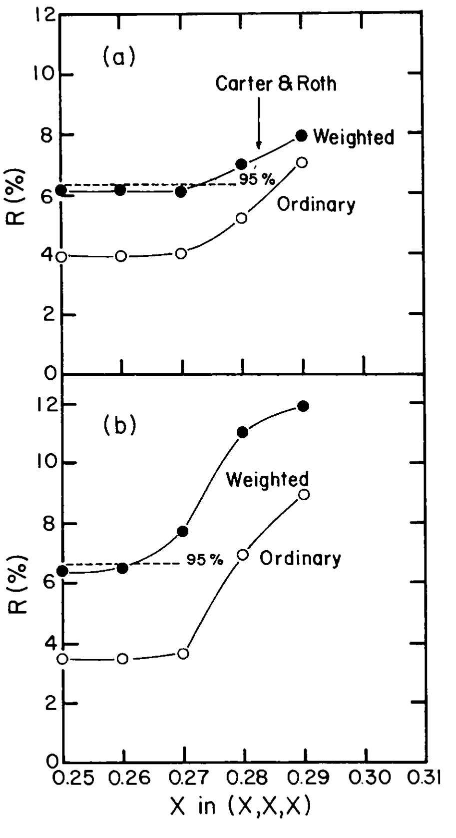

Fig. 2. Change in R with the displacement of oxygen ions along $\langle 111 \rangle$ directions. The position of displaced oxygen ions estimated by Carter & Roth (1968) is indicated by an arrow. The 95% confidence limits (Hamilton, 1965*b*) are shown. (*a*) $Zr(Ca)O_{2-x}$, (*b*) $Zr(Y)O_{2-x}$.

(iv) $\langle 100 \rangle$ *displacements of oxygen ions*

The refinement was continued for the scale factor, two isotropic temperature factors (for the cation and

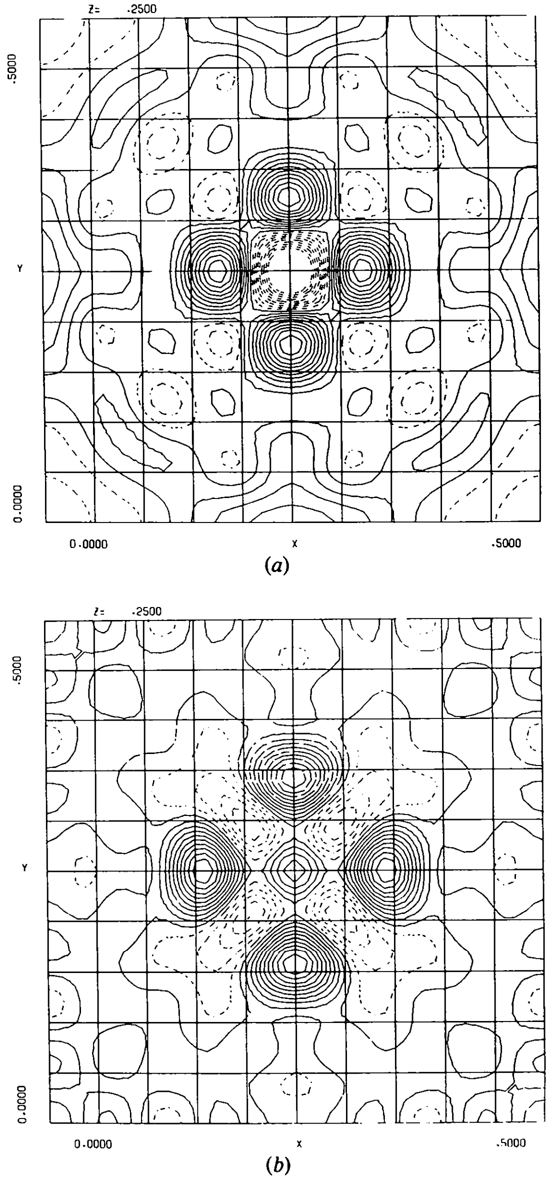

Fig. 3. Difference electron density maps at height $Z = \frac{1}{4}$ of (*a*) $Zr(Ca)O_{2-x}$, and (*b*) $Zr(Y)O_{2-x}$. The contour interval is 0·26 e Å^{-3} (*a*) and 0·15 e Å^{-3} in (*b*).

anion), and the number of displaced oxygen ions (with the total concentration of anions fixed), for a series of displacements of oxygen ions along the ⟨100⟩ directions. The results are shown in Fig. 4(*a*) for $Zr(Ca)O_{2-x}$, and (*b*) for $Zr(Y)O_{2-x}$. In these figures, the *R* values, the fraction of displaced and undisplaced oxygen ions and the two isotropic temperature factors (for the cations and the anion) are given. There are similar tendencies in these curves for both crystals.

For $Zr(Ca)O_{2-x}$, the *R* value shows a steep minimum near $x \simeq 0{\cdot}30$ (*i.e.* $\Delta/a \simeq 0{\cdot}05$) where the ordinary $R = 3{\cdot}41\%$, the weighted $R = 3{\cdot}57\%$, $B_C = 0{\cdot}803\ (15)\ \text{Å}^2$, $B_O = 1{\cdot}041\ (187)\ \text{Å}^2$ and 91·4 (6·2)% of the oxygen ions are displaced along the ⟨100⟩ directions. The magnitude of the displacement is $\Delta/a \simeq 0{\cdot}05$ ($\simeq 0{\cdot}256$ Å, as $a = 5{\cdot}1289$ Å).

On the other hand, for $Zr(Y)O_{2-x}$, the *R* value shows only a shallow minimum, near $x = 0{\cdot}30$, where the ordinary $R = 3{\cdot}49\%$, weighted $R = 5{\cdot}82\%$, $B_C = 1{\cdot}43\ (16)\ \text{Å}^2$, $B_O = 1{\cdot}152\ (101)\ \text{Å}^2$ and 60·6 (9·6)% of total oxygen ions are displaced along the ⟨100⟩ directions. The magnitude of displacement is again $\Delta/a \simeq 0{\cdot}05$ ($\simeq 0{\cdot}257$ Å; $a = 5{\cdot}1482$ Å).

A refinement of the displacements of oxygen ions along *both* the ⟨100⟩ and ⟨111⟩ directions was carried out, but the *R* values increased and the oxygen temperature factors became negative. Also, the present analysis was repeated using neutral scattering factors, and again there was no significant change in the results, or in the difference electron density maps.

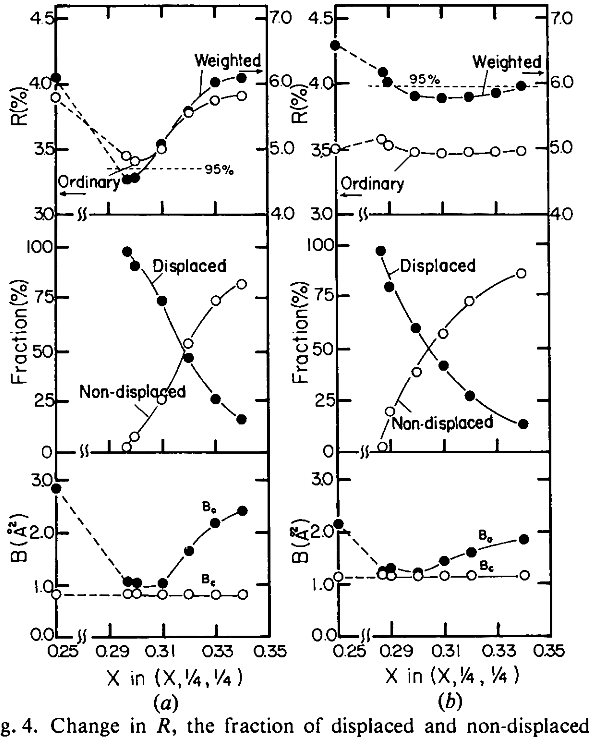

(*a*) (*b*)

Fig. 4. Change in *R*, the fraction of displaced and non-displaced oxygen ions, and the temperature factors of the cations (B_C) and the anion (B_O) with the displacement of oxygen ions along ⟨100⟩ directions. The 95% confidence limits (Hamilton, 1965*b*) are shown. (*a*) $Zr(Ca)O_{2-x}$, (*b*) $Zr(Y)O_{2-x}$.

The *R* value for $Zr(Y)O_{2-x}$ reduced further to 2·7% (weighted and unweighted) when small displacements ($\Delta/a \sim 0{\cdot}015$) were allowed for the cations in ⟨111⟩ directions in addition to the ⟨100⟩-type displacements of the anions. (Displacements along ⟨100⟩, ⟨110⟩ and ⟨111⟩ were attempted but the *R* values were unchanged.) This is in accord with suggestions by Steele & Fender (1974) for a similar material, $Zr(Yb)O_{0{\cdot}187}$, $\Delta x = 0{\cdot}22a$, but this was not the case for $Zr(Ca)O_{2-x}$.

Finally, a refinement including the occupation factors of all sites was attempted but this did not reduce the *R* values and there were large uncertainties in the resultant values.

Note in Fig. 4 that there are fewer undisplaced oxygen ions for $Zr(Ca)O_{2-x}$ at the minimum in *R* than for $Zr(Y)O_{2-x}$, as was indicated by the difference electron density maps in § (iii).

Discussion

Calcia and yttria stabilized zirconias are excellent conductors of anions at temperatures above 1173 K (Etsell & Flengas, 1970; Roth, 1975), and this appears to be due to the exchange of the anions with the large concentration of anion vacancies. The high temperature factor for the oxygen ions found without shifts in coordinates indicates that there are large static and/or dynamic displacements of oxygen ions from their ideal fluorite sites. This implies that the oxygen ion is loosely bound, aiding this hopping process. Steele & Fender (1974) interpreted this high displacement as due to a neighbouring oxygen vacancy. [It is noted that a high temperature factor has also been reported for Ag in the superionic conductor AgI (Burley, 1967).]

In the ordered phase (Faber, Mueller & Cooper, 1978), there are shears in one cube direction in each cell, compared to the disordered phase. But even in this case, there are domains. It is therefore likely that in the disordered phase the displacements are in different ⟨100⟩ type directions in different regions (all of which are quite small).

There are three well-defined polymorphs of ZrO_2: monoclinic, tetragonal and cubic phases. The monoclinic phase, which is stable below ~1273 K, can be described as a distortion of the cubic CaF_2 structure (Smith & Newkirk, 1965). At higher temperatures the tetragonal phase is stable, and it transforms to the cubic phase at ~2573 K. From the results by Teufer (1962), the tetragonal phase of ZrO_2 can be described as resulting from the displacement of anions from the cubic fluorite positions along ⟨100⟩ directions. The magnitude of the displacement is $\Delta/a \simeq 0{\cdot}065$ when the cubic phase is taken as a reference. (Teufer reported $B_C = 1{\cdot}66$ and $B_O = 3{\cdot}11\ \text{Å}^2$ at 1523 K, which also

Table 2. *Examination of the fourth-order anharmonic contribution to Bragg peaks in stabilized zirconia*

hkl	$h^2+k^2+l^2$	$Zr(Ca)O_{2-x}$ Intensity	$[h^4+k^4+l^2$ $-3/5(h^2+k^2+l^2)^2]$	$Zr(Y)O_{2-x}$ Intensity
$h+k+l=4n+2$				
442 600	36	$I_{442} = I_{600}$	−249·6 +518·4	$I_{442} \geq I_{660}$
644 820	68	$I_{644} \geq I_{820}$	−1478·40 +1337·6	$I_{644} \geq I_{820}$
860 10,0,0	100	$I_{860} \geq I_{10,0,0}$	−608 +4000	$I_{860} \geq I_{10,0,0}$
882 10,4,4	132	$I_{882} \geq I_{10,4,4}$	−2246·4 +57·6	$I_{882} \geq I_{10,4,4}$
$h+k+l=4n$				
882 660	72	$I_{822} \geq I_{660}$	−12009·6 −13545·6	$I_{822} \leq I_{660}$
10,2,0 862	104	$I_{10,2,0} \geq I_{862}$	+3526·4 −1081·6	$I_{10,2,0} \leq I_{862}$
10,6,0 866	136	$I_{10,6,0} \geq I_{866}$	+198·4 −7001·6	$I_{10,6,0} \leq I_{866}$
12,0,0 884	144	$I_{12,0,0} \geq I_{884}$	+8294·4 −3993·6	$I_{12,0,0} \leq I_{884}$
12,2,2 10,6,4	152	$I_{12,2,2} \geq I_{10,6,4}$	+6905·6 −2310·4	$I_{12,2,2} \leq I_{10,6,4}$

suggests that ⟨100⟩ anion displacements may be present even in pure ZrO_2.) It is interesting that this displacement mode for tetragonal ZrO_2 is coincident with that in the ordered $Zr(Ca)O_{2-x}$ reported by Faber, Mueller & Cooper (1978). These authors, and Cooper (1978), searched for the particular internal displacements of anions such that the net elastic force on the undistorted cation sites vanishes, and found a ⟨100⟩ displacement mode of oxygen ions, with $\Delta/a \simeq 0{\cdot}044$ in ordered $Zr(Ca,Y)O_{2-x}$. On the other hand, Steele & Fender (1974) reported $\Delta/a = 0{\cdot}073$ for disordered $Zr(Y)O_{1{\cdot}87}$. Thus, the ⟨100⟩ displacement in the disordered phase may well be a precursor to the ordering reaction, and related to the transformations in pure ZrO_2.

It is of interest to consider whether the observed anion displacements are due to anharmonic interactions, or are static in nature. It is well known (see, for example, Willis & Pryor, 1975) that third-order anharmonic interactions affect only the anions in these materials (sites with $\bar{4}3m$ symmetry in the fluorite structure). For reflections with the same $h^2 + k^2 + l^2$ but with $h + k + l = 4n + 1$ or $4n - 1$, the effect is different. This is not the case, as can be seen in Fig. 1. Furthermore, such third-order coupling must result in displacements in ⟨111⟩ directions in this structure and this is not what has been found here. The ⟨100⟩ type displacements that we have detected could be due to fourth-order interactions. The term that appears in the Debye–Waller factor for such interactions is: $C[(h^4 + k^4 + l^4) - \frac{3}{5}(h^2 + k^2 + l^2)^2]$. This value is presented in Table 2 for pairs of reflections with the same $h^2 + k^2 + l^2$, along with their relative intensities for both crystals. If there were no anharmonic interactions, each pair would have the same intensity. On the other hand, for this fourth-order anharmonic interaction it would be expected that reflections having negative values of this term would all be larger (for C negative) or all smaller (for C positive), than for the positive values for $h + k + l = 4n + 2$; the reverse would be true for $h + k + l = 4n$, since the anion contribution to the structure factor is opposite in sign for these two classes of reflection. This appears to be the case (C negative) for $Zr(Ca)O_{2-x}$, but not for $Zr(Y)O_{2-x}$. Perhaps there are different reasons for the effects in the two materials, but in view of their other similarities this seems doubtful. Furthermore, the large concentrations of defects undoubtedly leads to defect interactions, and therefore we suggest that these effects are due to static displacements.

We are grateful to T. H. Etsell for lending us the crystals used in this study. (These were not from the same batch used by Faber, Mueller & Cooper, 1978.) This research was supported at Northwestern University by the US Army Research Office under Grant No. DAAG 29-76-G-0303. The X-ray work was carried out in the Long Term X-ray Facility of Northwestern University's Materials Research Center, supported in part by NSF through Grant No. DMR-76-80847. One of us (JF) acknowledges the support of the Department of Energy and Argonne National Laboratory where initial X-ray studies were performed.

References

ALLPRESS, J. G. & ROSSEL, H. J. (1975). *J. Solid State Chem.* **15**, 68–78.

ALLPRESS, J. G., ROSSEL, H. J. & SCOTT, H. G. (1975). *J. Solid State Chem.* **14**, 264–273.

BUERGER, M. J. (1960). *Crystal Structure Analysis*. New York: John Wiley & Sons.

BURLEY, G. (1967). *J. Phys. Chem. Solids*, **25**, 629–634.

BUSING, W. R., MARTIN, K. O. & LEVY, H. A. (1960). *ORFLS*, Report ORNL-TM-305. Oak Ridge National Laboratory, Oak Ridge, Tennessee.

CARTER, R. E. & ROTH, W. L. (1963). General Electric Res. Rep. No. 63-RL-3479 M.

CARTER, R. E. & ROTH, W. L. (1968). *Electromotive Force Measurements in High-Temperature Systems*, edited by C. R. ALCOCK, pp. 125–144. The Institute of Mining and Metallurgy, New York.

COOPER, B. R. (1978). *Phys. Rev. B*, **17**, 293–296.

CORFIELD, P. W. R., DOEDENS, D. J. & IBERS, J. A. (1967). *Inorg. Chem.* **6**, 197–204.

DINESS, A. M. & ROY, R. (1965). *Solid State Commun.* **3**, 123–125.

ETSELL, T. H. & FLENGAS, S. N. (1970). *Chem. Rev.* **20**, 339–376.

FABER, J. JR, MUELLER, M. H. & COOPER, B. R. (1978). *Phys. Rev. B*, **17**, 4884–4888.

HAMILTON, W. C. (1965*a*) *Trans. Am. Crystallogr. Assoc.* **1**, 17–26.

HAMILTON, W. C. (1965*b*). *Acta Cryst.* **18**, 502–510.
HUDSON, B. & MOSELEY, P. T. (1976). *J. Solid State Chem.* **19**, 383–389.
International Tables for X-ray Crystallography (1974). Vol. IV. Birmingham: Kynoch Press.
RICHESSON, M., MORRISON, L., COHEN, J. B. & PAAVOLA, K. (1971). *J. Appl. Cryst.* **4**, 524–527.
ROTH, W. L. (1975). *Crystal Structure and Chemical Bonding in Inorganic Chemistry*, edited by C. J. M. ROOYMANS & A. RABENAV, pp. 85–102. Amsterdam: North-Holland.
SARDI, O. (1969). PhD Thesis, Univ. of Indiana.
SCHWARTZ, L. H. & COHEN, J. B. (1977). *Diffraction from Materials*, pp. 191–192. New York: Academic Press.
SMITH, D. K. & NEWKIRK, H. W. (1965). *Acta Cryst.* **18**, 983–991.
STEELE, D. & FENDER, B. E. F. (1974). *J. Phys. C*, 7, 1–11.
TEUFER, G. (1962). *Acta Cryst.* **15**, 1187.
TOKONAMI, M. (1965). *Acta Cryst.* **19**, 486.
WILLIS, B. T. M. & PRYOR, A. W. (1975). *Thermal Vibrations in Crystallography*, pp. 142–159. London: Cambridge University Press.

Acta Cryst. (1979). A**35**, 795–802

Intensity Errors due to Beam Inhomogeneity and Imperfectly Spherical Crystals

BY H. D. FLACK AND M. G. VINCENT

Laboratoire de Cristallographie aux Rayons X, 24, *quai Ernest Ansermet, Université de Genève,*
CH-1211 *Genève* 4, *Switzerland*

(*Received* 19 *February* 1979; *accepted* 28 *March* 1979)

Abstract

An analysis of the intensity errors from imperfectly spherical crystals with an inhomogeneous incident X-ray beam is presented. The crystals are considered to have either no absorption or strong absorption. The inhomogeneity of the incident beam profile is represented by three possible models: (*a*) a Lorentzian, (*b*) a Gaussian and (*c*) a second-order Taylor series expansion. The results are compared with intensities for electron density studies from five crystals.

1. Introduction

The necessity for precise intensity measurements of X-rays diffracted by a crystal has increased with the interest in electron density studies. The conditions which must be met to obtain useful results from metallic systems are more restrictive than those in light atom systems due to the presence of absorption in the material. A common approach to reducing systematic errors in heavy-atom systems is to try to prepare a sample in the form of a sphere. However, the shapes of crystals obtained are seldom truly spherical. In a previous publication (Vincent & Flack, 1979*a*), we have estimated the intensity variations among equivalent reflections due to absorption to be expected from imperfectly spherical crystals. The predicted intensity variations seem to be smaller than those currently obtained in a real experiment. We have thus been drawn to analyse the effects due to beam inhomogeneity and crystal miscentring jointly with absorption from imperfectly spherical crystals.

2. Relationship between intensity and shape variations

In order to investigate changes in diffracted intensity due to variations in shape, we need to calculate the total intensity (energy) diffracted by a crystal of given shape and then derive intensity changes for changes in shape. The integrated reflection intensity, ρ, from an infinitesimally small block of volume δV of a crystal is given by

$$\rho = Q\,\delta V, \tag{1}$$

where Q contains the Lorentz–polarization factors, structure amplitude squared and some fundamental physical constants (*International Tables for X-ray Crystallography*, 1967). ρ is related to the total amount of energy diffracted (E) by

$$\rho = E\omega/I_0, \tag{2}$$

where ω is the angular velocity of rotation of the crystal and I_0 is the intensity of the incident X-radiation falling normally on unit area per unit time. Combining (1) and (2) we find

$$E = (Q/\omega)\,I_0\,\delta V. \tag{3}$$

For a particular reflection under fixed measuring conditions, Q/ω is a constant. The total energy diffracted by a finite crystal may be obtained by

0567-7394/79/050795-08$01.00